Development 136, 1977-1986 (2009) doi:10.1242/dev.030718

Myosin II regulates extension, growth and patterning in the mammalian cochlear duct

Norio Yamamoto[1], Takayuki Okano[1], Xuefei Ma[2], Robert S. Adelstein[2] and Matthew W. Kelley[1,*]

The sensory epithelium of the mammalian cochlea comprises mechanosensory hair cells that are arranged into four ordered rows extending along the length of the cochlear spiral. The factors that regulate the alignment of these rows are unknown. Results presented here demonstrate that cellular patterning within the cochlea, including the formation of ordered rows of hair cells, arises through morphological remodeling that is consistent with the mediolateral component of convergent extension. Non-muscle myosin II is shown to be expressed in a pattern that is consistent with an active role in cellular remodeling within the cochlea, and genetic or pharmacological inhibition of myosin II results in defects in cellular patterning that are consistent with a disruption in convergence and extension. These results identify the first molecule, myosin II, which directly regulates cellular patterning and alignment within the cochlear sensory epithelium. Our results also provide insights into the cellular mechanisms that are required for the formation of highly ordered cellular patterns.

KEY WORDS: Hair cell, Organ of Corti, Inner ear, Pillar cell, Mouse

INTRODUCTION

In mammals sounds are perceived by the organ of Corti (OC), a sensory epithelium that extends along the basal-to-apical axis of the cochlear spiral. The OC comprises highly ordered rows of mechanosensory hair cells and non-sensory supporting cells. The evolution of an elongated cochlea and the unique morphology of the OC represent key steps in the evolution of the ability to perceive and discriminate a wide range of auditory frequencies (von Bekesy, 1949). The mechanisms that regulate elongation of the duct and/or cellular patterning within the OC are largely unknown. However, it has recently been suggested that convergence and extension, mediated at least in part through the planar cell polarity (PCP) pathway, plays a role in both cochlear elongation and cellular patterning (Chen et al., 2002; Montcouquiol et al., 2003; McKenzie et al., 2004; Wang et al., 2005; Qian et al., 2007). Convergent extension (CE) refers to a morphogenetic process in which the three-dimensional distribution of a population of cells extends along one axis while simultaneously narrowing along a perpendicular axis (Keller et al., 2000; Keller, 2002). In some cases, CE can be preceded by a period of radial intercalation in which cells extend as a result of thinning along an axis oriented perpendicular to the axes of subsequent CE (Keller, 2000; Keller et al., 2002). CE has been observed during amphibian gastrulation (Keller, 1986) and neurulation (Jacobson and Gordon, 1976) and more recently in *Drosophila* germband extension (Irvine and Weischaus, 1994).

Non-muscle myosin 2 (NM II) is a hexameric protein composed of two dimeric heavy chains (NMHCs), a pair of regulatory light chains (RLCs) and a pair of essential light chains. Phosphorylation of the RLCs by a number of kinases, principally myosin light chain kinase (Kamm and Stull, 1985) and RHO-associated protein kinase (ROCK) (Amano et al., 1996; Conti and Adelstein, 2008), regulates self-assembly and ATPase activity (Conti and Adelstein, 2008). Recently, myosin II has been shown to play a significant role in CE in both *Drosophila* and vertebrates (Sellers, 2000; Bertet et al., 2004; Conti and Adelstein, 2008; Skoglund et al., 2008). The specific effects of NM II during CE are still poorly understood but can include junctional remodeling and changes in cell shape (Conti and Adelstein, 2008).

In humans and mice three genes encode NMHC II, *MYH9*, *MYH10* and *MYH14* (Golomb et al., 2004). Although a role for NM II in cochlear development has not been reported, both syndromic and non-syndromic hearing loss results from mutations in MYH genes, including *R702H*, *R702C* and *R705H* mutations in *MYH9* (Lalwani et al., 2000; Heath et al., 2001) and *S7X*, *S120L*, *G376C* and *R726S* mutations in *MYH14* (Donaudy et al., 2004; Yang et al., 2005). The physiological basis for the auditory defect in these individuals has not been determined, but is believed to be sensorineural in nature (Chen et al., 1995; Lalwani et al., 1997). Based on these results, it seemed likely that myosin II could play an important role in cellular patterning and/or extension of the OC during embryonic development.

MATERIALS AND METHODS

Animals

ICR mice were purchased from Charles River Laboratories. *Myh9, Myh10* and *Myh14* null and $Myh10^{DN}$ mice were described previously (Tullio et al., 1997; Conti et al., 2004; Ma et al., 2004). To restrict expression of $Myh10^{DN}$ to the developing ear, the $Foxg1^{Cre}$ line (Hebert et al., 2000) was used to remove the neomycin cassette in the otocyst, forebrain and retina. Resulting embryos survived until E16.5 and were obtained in expected ratios. All animals were maintained based on the standards outlined in the National Institutes of Health Guide for the Care and Use of Laboratory Animals.

Determination of changes in cochlear length and cellular patterning

Cochleae were dissected from embryos at specific developmental time points, the developing cochlear epithelium was exposed and cell boundaries and prosensory cells were labeled with phalloidin and anti-$p27^{Kip1}$ (CDKN1B - Mouse Genome Informatics) as previously described (McKenzie et al., 2004). Changes in length and width of the prosensory domain were determined as previously described (McKenzie et al., 2004). To determine changes in individual cell shape, 150 μm of cochlear sensory epithelia located at the 50% position along the basal-to-apical axis of the cochlea length was imaged.

[1]Section on Developmental Neuroscience, National Institute on Deafness and other Communication Disorders, and [2]Laboratory of Molecular Cardiology, Genetics and Developmental Biology Center, National Heart Lung and Blood Institute, National Institutes of Health, Bethesda, MD 20892, USA.

*Author for correspondence (e-mail: kelleymt@nidcd.nih.gov)

Accepted 6 April 2009

ImageJ (http://rsb.info.nih.gov/ij/) and Metamorph (Universal Imaging) software packages were used to determine the length, width and area of each cell within the region. A minimum of three separate cochleae from different litters were analyzed for each time point. Changes in the number of specific cell types were determined by labeling cell boundaries with phalloidin and labeling cells with specific markers such as anti-myosin 6 for hair cells and anti-p75^{NTR} (NGFR – Mouse Genome Informatics) for pillar cells.

Reverse transcriptase polymerase chain reaction

Epithelia from five E13.5 or E16.5 cochleae were isolated by treating with thermolysin (Montcouquiol and Kelley, 2003) and total RNA was extracted. cDNA was synthesized using the ABI cDNA Synthesis Kit (Applied Biosystems, Foster City, CA, USA). Sequences for primer sets for *Myh9*, *Myh10* and *Myh14* are available upon request.

Quantitative RT-PCR

Total RNA was prepared as described above. For experiments using *Myh10* null mice, total RNA was extracted from two cochlear epithelia for each genotype. cDNA was mixed with Power SYBR Green PCR Master Mix (Applied Biosystems) and subjected to real-time PCR quantification using an ABI PRISM 7000 Sequence Detection System (Applied Biosystems). All reactions were performed in triplicate. The relative amounts of mRNAs were calculated by using the standard curve method. As the invariant control, we used mouse *Arbp* (*Rplp0* – Mouse Genome Informatics) mRNA (Yabe et al., 2003). Sequences for primer sets are available upon request.

Immunohistochemistry

For whole mounts, cochleae were prepared as described in Jacques et al. (Jacques et al. 2007). For immunohistochemical analysis of sections, cochleae were dissected, fixed in 4% paraformaldehyde, cryoprotected through a sucrose gradient, embedded in Tissue-Tek (MILES, Elkhart, Illinois, USA) and sectioned on a cryostat.

Primary antibodies were: rabbit anti-MYH9 and anti-MYH10 (1:500, polyclonal, Covance); rabbit anti-MYH14 [1:500, polyclonal (Golomb et al., 2004)]; rabbit anti-myosin 6 (1:1000, polyclonal, Proteus BioSciences); rabbit anti-p27^{Kip1} (1:100, polyclonal, Lab Vision); and rabbit anti-p75^{NTR} (1:1000, polyclonal, Chemicon). Specificity of anti-MYH9, anti-MYH10 and anti-MYH14 antibodies were confirmed by western blot (see Fig. S1 in the supplementary material). Actin filaments were visualized with Alexa488-conjugated phalloidin (1:200, Invitrogen-Molecular Probes).

Primary antibodies were visualized with Alexa488- or Alexa546-conjugated secondary antibodies (Invitrogen-Molecular Probes). All fluorescent images were obtained on an LSM510 laser scanning microscope (Carl Zeiss).

Determination of changes in orientation of cell-cell boundaries

Cochleae from E14 embryos were labeled with phalloidin as described. Developing hair cells were identified based on increased accumulation of actin (McKenzie et al., 2004). Cells located within 7 μm of the medial edge of the inner hair cells were classified as within the pillar cell domain and cells located between 7 and 14 μm from the medial edge of inner hair cells were classified as within the outer hair cell region. All of the cell-cell boundaries located along at least 50 μm of the basal-to-apical axis were included for each sample and a minimum of three separate cochleae were included for each location.

Assessment of cochlear extension

Cochleae were dissected from mouse embryos at E14. Following dissection, the cochlear duct was cut at the midpoint and the basal half was established as an explant culture. Explants were maintained for 4 days in vitro. At the end of each experiment, hair cells were labeled with anti-myosin 6 and the extent of outgrowth and change in width of the sensory epithelium was determined based on the distribution of hair cells. A minimum of seven explants from multiple litters were analyzed for each control or experimental group.

Cochlear explant cultures

Cochleae were isolated as described above except the epithelium was left intact. In order to visualize the sensory epithelium, the roof of the duct was removed. Explants were maintained as described previously (Montcouquiol et al., 2003). For cultures containing just the developing cochlear epithelium, cochleae were dissected as described and the epithelium was isolated by treatment with thermolysin (Montcouquiol et al., 2003). The length and width of the sensory epithelium was determined as described for the outgrowth assay.

Inhibition of NM II function in vitro

Cochlear explants were treated with 3 or 10 μM of blebbistatin (Sigma-Aldrich) or Y27632 (EMD Chemicals), plus 0.1% DMSO as a vehicle. Control explants were treated with vehicle alone.

RESULTS

The cochlear sensory epithelium extends between E14 and E16

The sensory epithelium of the mammalian cochlea originates in the basal region of the cochlear spiral located near the oval window and continues as a narrow strip of cells to the apex located at the tip of the coil (apicobasal axis). The width of the epithelium is measured along the mediolateral axis oriented perpendicular to the apicobasal axis. At any point along the cochlea, the thickness of the epithelium spans from the basement membrane to the lumenal surface (basolumenal axis). Previous results have demonstrated that the developing sensory epithelium undergoes significant extension between E14 and E16, with E16 representing the earliest time at which the final cellular pattern of the OC can be identified (Cantos et al., 2000; McKenzie et al., 2004). To confirm these results, prosensory cells were identified based on expression of p27^{Kip1} (Chen and Segil, 1999) and the overall dimensions of the prosensory domain were determined at E14 and E16. Results indicated changes in the length and width of the prosensory domain (Fig. 1A-C) that are consistent with convergence and extension as suggested by Chen and Segil (Chen and Segil, 1999) and McKenzie et al. (McKenzie et al., 2004).

Changes in cell shape correlate with extension of the cochlear duct

To determine changes in individual cell shapes during the E14 to E16 period of extension, the lumenal dimensions of each prosensory cell were identified by labeling cortical actin with phalloidin (Fig. 1D,E). Average lumenal morphologies for over 500 prosensory cells were determined in a region of the cochlear duct located at the midpoint along the apicobasal axis of the cochlea. At E14, the majority of prosensory cells have rounded lumenal profiles with a length (measured along the apicobasal axis) to width (measured along the mediolateral axis) ratio of ~1.4 and an average lumenal surface area of ~5.0 μm^2 (Fig. 1F). By E16, lumenal surfaces have significantly increased both in length and in width leading to a doubling in the average surface area. In addition, there is a small but significant increase in the length/width ratio, indicating a disproportionate lengthening of each cell. The observation that individual cell width actually increases between E14 and E16, while the overall width of the sensory epithelium decreases, suggests that the data in Fig. 1 probably underestimate the amount of convergence that occurs. Finally, the increase in the lumenal surface area of each cell, along with the decrease in the width of the sensory epithelium, results in a significant decrease in the density of prosensory cells along both the apicobasal and proximodistal axes (Fig. 1F).

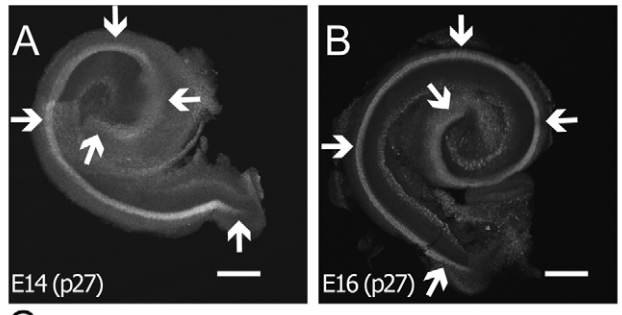

C Sensory Epithelium

	Average Length (μm)	Average Width (μm)	Length/Width	Average Area (μm²)
E14	1,984.5 ± 87.6	35.6 ± 2.2	55.8 ± 1.6	70,773.0 ± 7,248.7
E16	3,398.9 ± 158.5*	25.2 ± 2.8*	136.8 ± 19.6*	85,230.3 ± 5,842.1**

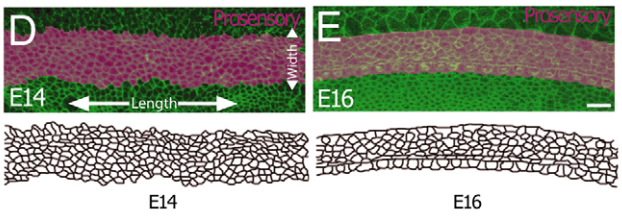

F Sensory Cells

	E14	E16
Average Length (μm)	3.3 ± 0.8	4.8 ± 1.2***
Average Width (μm)	2.4 ± 0.7	3.3 ± 0.8***
Length/Width	1.4 ± 0.5	1.5 ± 0.5***
Average Surface Area (μm²)	5.0 ± 2.2	10.2 ± 4.2***
Average Density/ 100 μm Length	305.9 ± 44.3	156.8 ± 11.0**
Average Density/ Width of SE	17.6 ± 1.5	10.7 ± 1.3**

Fig. 1. Convergence and extension of the cochlear prosensory domain. (**A**,**B**) Whole mounts of the cochlea at E14 (A) and E16 (B). The prosensory domain is marked by expression of $p27^{Kip1}$ (arrows). Note the extension and narrowing of the prosensory domain (arrows) that occurs between E14 and E16. (**C**) Comparison of changes in length, width, length/width ratio and surface area of the sensory epithelium between E14 and E16. There is a significant increase in length, a significant decrease in width and a significant increase in overall area. (**D**,**E**) Phalloidin labeling (green) of cell-cell boundaries in the cochlear duct. The prosensory domain is illustrated in violet. Arrows in D indicate orientation of length and width axes. The lower aspect of each panel illustrates outlines for individual cells within the prosensory domain. (**F**) Comparison of changes in length, width, length/width ratio, surface area, and cell density per unit length and across the width of the sensory epithelium between E14 and E16. The decrease in density of cells along the width of the epithelium is consistent with ongoing convergence. Scale bars: 200 μm in A,B; 10 μm in E (same magnification in D). *P<0.005, **P<0.05, ***P<0.0001.

Myh9, Myh10 and *Myh14* are expressed in the cochlear epithelium

The data presented above suggested a role for CE and growth during the development of the OC. To determine whether NM II plays a role in these events, the expression of mRNA for all three NMHCs within the developing sensory epithelium was determined. Results of RT-PCR analysis indicated that, in addition to other tissues, all three MYH genes are expressed in the cochlear epithelium at both E13.5 and E16.5 (see Fig. S2 in the supplementary material). None of the reported splice variants of *Myh10* (Itoh and Adelstein, 1995) was observed in the cochlea, but all of the splice variants for *Myh14* (Golomb et al., 2004) were present.

Next, developmental changes in the level of expression of each MYH gene within the cochlea were determined by quantitative RT-PCR (see Fig. S2 in the supplementary material). Expression of *Myh9* steadily decreased between E12.5 and E16.5. Expression of *Myh10* also decreased during the same time period, but the relative level of decrease was less than for *Myh9*. By contrast, expression of *Myh14* increased nearly sixfold between E12.5 and E16.5. This result is consistent with previous results showing that *Myh14* is more abundant in adult tissues (Golomb et al., 2004).

MYH10 and MYH14 are asymmetrically distributed in developing cochlear sensory epithelial cells

To determine the cellular and subcellular distribution of each of the MYH proteins within the developing cochlea, immunohistochemical localization was carried out in both whole mounts and cryostat sections at E13.5 and E16. MYH9 immunoreactivity is limited and diffuse throughout the cochlea at both time periods (see Fig. S3 in the supplementary material) although MYH9 is observed in other tissues, such as the neural tube. By contrast, at E13.5 MYH10 and MYH14 are distributed uniformly around the lumenal surface in all cells of the developing sensory epithelium (data not shown). To examine the change in distribution of MYH10 and MYH14 during the period of cochlear extension, the localization of both proteins was studied in E16 cochleae. The sensory epithelium of the cochlea develops in a gradient that extends from base to apex. At E16, the sensory epithelium at the base of the cochlea is comparatively mature with a recognizable pattern of hair cells and supporting cells. By contrast, the apex of the cochlea at E16 appears undifferentiated with no obvious cellular patterning. Therefore, changes in developmental distribution of MYH proteins could be examined in a single cochlea. In the undifferentiated apex of the cochlea, MYH10 distribution is largely homogenous, with a slight increase in expression that forms a faint line oriented along the apicobasal axis and located near the medial boundary of the sensory epithelium (Fig. 2A). In the mid-apical and middle regions of the cochlea, two lines of MYH10 are obvious, one (continuous with the faint line observed in the apical region) that correlates with the boundary between inner hair cells and inner pillar cells (IPCs) and a second one located at the apparent lateral boundary of the sensory epithelium (see Fig. 2B for explanation of cellular patterning in the OC). In the mid-basal region, a third line of MYH10, located between the IPCs and the first row of outer hair cells, is apparent. In addition, the distance between the first two lines of MYH10 is decreased (from an average of 10.06 μm to 7.56 μm), consistent with convergence of the sensory epithelium. Finally, in the basal region, the three lines of MYH10 persist and the distance between the first and second lines is decreased even further. Moreover, additional lines of MYH10, also oriented along the axis of extension (apicobasal axis), are present between the rows of developing outer hair cells.

In contrast to MYH10, in E16 cochleae MYH14 is predominantly localized to the developing IPCs, inner hair cells and inner phalangeal cells. In the apical and mid-apical regions, MYH14 is uniformly distributed throughout the sensory epithelium, however, more prominent labeling is present on the medial edges of developing IPCs, resulting in a line oriented along the axis of extension (Fig. 2C). In the middle and mid-basal regions, MYH14 labeling is decreased in the outer hair cell region, but becomes more prominent in the IPC and inner hair cell regions. Finally, in the mature basal region, MYH14 is prominently distributed in IPCs and inner phalangeal cells and might also be expressed in inner hair cells. By contrast, labeling is almost completely absent in the outer hair

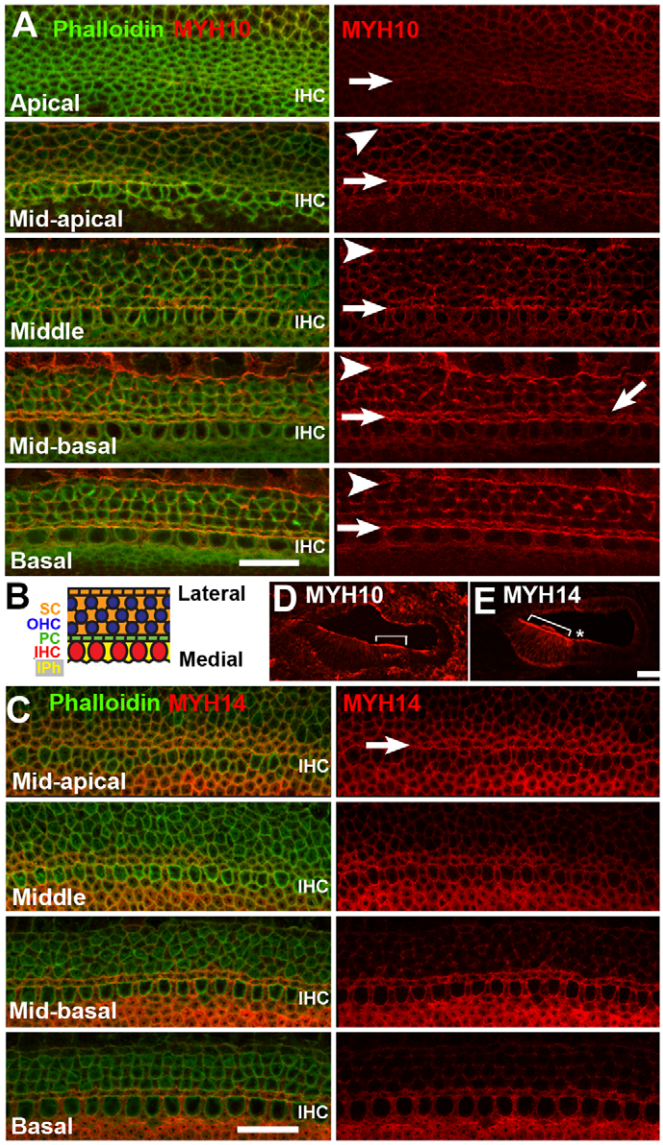

Fig. 2. Distribution of MYH10 and MYH14 along the basal-to-apical axis of the cochlea at E16.5. (**A**) In the apical region, MYH10 distribution (red) is largely uniform at all cell boundaries, with the exception of a faint line of increased intensity (arrow) near the medial edge of the sensory epithelium (see Fig. 2B for diagram of cellular pattern in mature OC). The position of developing inner hair cells (IHC) is indicated for orientation. In the mid-apical and middle regions, two lines are present, a line located between IHCs and IPCs (arrow) that is continuous with the line in the apical region, and a second line located at the extreme lateral edge of the OC (arrowhead). In the mid-basal region, a third line located at the boundary between IPCs and OHCs is also present (angled arrow). In the basal region shorter lines are also present between each row of OHCs. (**B**) Diagram illustrating the cellular pattern in the OC. (**C**) Distribution of MYH14 (red). In the mid-apical region, MYH14 is uniformly distributed with slightly brighter labeling at the boundary between IHCs and IPCs (arrow). In more mature regions, MYH14 is prominent at all boundaries of PCs, IHCs and IPhs but labeling is considerably reduced in the OHC region. (**D**,**E**) Cross-sections through the cochlear duct at E16.5 illustrating the distribution of MYH10 (D) and MYH14 (E). Bracket indicates the sensory epithelium in D and Kolliker's organ in E. Asterisk in E indicates the sensory epithelium. IHC, Inner hair cell; IPh, Inner phalangeal cell; IPC, Inner pillar cell; OPC, Outer pillar cell; OHC, Outer hair cell; SC, Supporting cell. Scale bars: 10 μm in A,C; 15 μm in E (same magnification in D).

cell region. Specificity of each antibody was confirmed by western blot and no primary control (see Figs S1 and S3 in the supplementary material).

Cell shape changes in the sensory epithelium are consistent with convergence and extension

The marked distribution of MYH10 and MYH14 in developing IPCs suggested that these cells might play an important role in cochlear CE. Previous results suggest that changes in cell shape, and in particular increased length along the axis of elongation, provide at least some of the driving forces for CE (Bertet et al., 2004). The initial analysis of changes in cell shape within the developing sensory epithelium between E14 and E16 had indicated only minor changes in the overall length/width ratio for all cells within the sensory epithelium (Fig. 1F). However, during this analysis, a subset of cells with elongated axes oriented parallel to the direction of elongation were observed adjacent to developing inner hair cells, a position consistent with the location of developing IPCs (Fig. 3A). To determine whether these elongated cells might indicate a region of ongoing extension, the total length of cell-cell contacts oriented parallel, perpendicular or intermediate to the axis of elongation was determined (Fig. 3B,C). For comparison, cells located in different regions of the epithelium, or in the same region but at an earlier time point, were also analyzed. Results indicated that cells located adjacent to developing inner hair cells undergo a significant change in cell shape that includes lengthening along the apicobasal axis of the cochlea and shortening along the medial-to-lateral axis. Cells located slightly farther from the developing inner hair cell region, but still within the developing sensory epithelium, showed similar but less pronounced cell shape changes, whereas cells located medial to the sensory epithelium did not change shape.

Expression of dominant negative *Myh10* inhibits extension and disrupts cellular patterning in the cochlea

To determine whether myosin II plays a role in cochlear extension, mice with targeted mutations in each of the MYH genes were analyzed. Deletion of *Myh9* results in embryonic lethality at E7.5 (Conti et al., 2004). Since this is well before the onset of cochlear development, no analysis of cochlear extension was possible in *Myh9* mutants. By contrast, *Myh10* null mice survive until E15 (Tullio et al., 1997) and *Myh14* null mice are viable. However, no defects were observed in the length or overall morphology of the cochleae in either mutant (data not shown). Considering that all three MYH proteins are expressed in the embryonic cochlea, functional or genetic compensation, as has been reported in the embryonic heart (Tullio et al., 1997), seemed possible. Although quantitative PCR for *Myh14* in *Myh10* mutants indicated no change in the level of *Myh14* expression (data not shown), compensation at post-transcriptional levels cannot be ruled out.

Therefore, to examine the effects of reduced MYH function, we analyzed cochleae from mice carrying a putative dominant negative mutation (R709C) in *Myh10* (Ma et al., 2004). Previous studies have demonstrated that mutations in the conserved R709 residue compromise actin-activated MgATPase activity and in vitro motility, as well as inhibiting the activity of wild-type MYHs (Kim et al., 2005). Activation of the $Myh10^{R709C}$ mutation (referred to as $Myh10^{DN}$) in the inner ear was accomplished using $Foxg1^{Cre}$ (see Materials and methods for details). The resulting $Myh10^{DN/DN};Foxg1^{Cre/+}$ mice survived until E16.5 and were obtained at expected mendelian ratios.

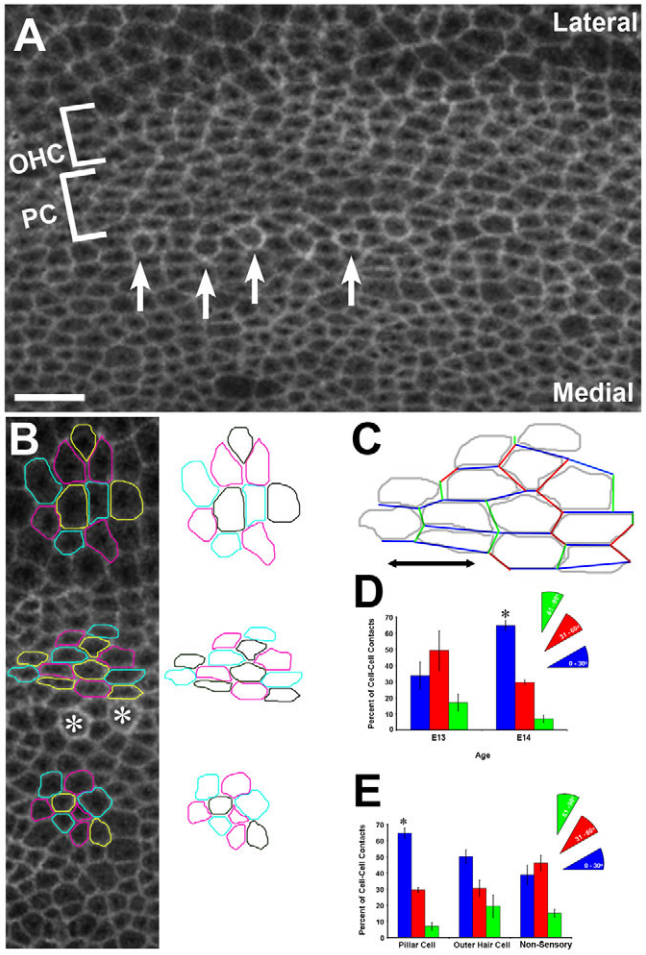

Fig. 3. Developing pillar cells undergo cell shape changes that are consistent with CE. (**A**) Middle region of the cochlea at E14. Cells located in the developing pillar cell (PC) and outer hair cell (OHC) domains, adjacent to developing inner hair cells (arrows), appear flattened. (**B**) Outlines of individual cells (colored for clarity) in three different regions of the cochlea. See A for orientation. Cells located adjacent to developing inner hair cells (asterisks) are flattened in comparison with cells located medial or lateral to the developing sensory epithelium. (**C**) Cell boundaries were classified as either parallel (0° to 30°, blue), perpendicular (61° to 90°, green) or intermediate (31° to 60°, red) to the axis of extension (black two-headed arrow). (**D**) Comparison of the ratios of different orientations of cell boundaries, as described in C, within the sensory epithelium between E13 and E14. Parallel boundaries are increased at the expense of intermediate and perpendicular boundaries. (**E**) Comparison of cell boundaries as in D, in different regions within the same cochlea at E14. A significantly greater proportion of cell-cell boundaries are oriented parallel to the axis of extension in the pillar cell region as compared with a non-sensory region. The outer hair cell region shows a similar distribution of boundary orientations, but values were not significantly different from the non-sensory region. Data for E14 pillar cell region are the same as for E14 in D. Scale bar: 10 μm. *P<0.01.

To determine whether myosin II regulates extension, the length and width of the prosensory domain was determined in experimental ($Myh10^{DN/DN}$;$Foxg1^{Cre/+}$) and control ($Myh10^{+/+}$;$Foxg1^{Cre/+}$) cochleae at E16 (Fig. 4A-D). Results indicated a significantly shorter prosensory domain in the cochleae of experimental versus control embryos (Fig. 4E). A corresponding increase in the width of the prosensory domain was not observed in experimental cochleae, except in the apex (Fig. 4B). However, the average lumenal surface of prosensory cells was significantly reduced (Fig. 4E), whereas the density of cells along the basal-to-apical axis was significantly increased (Fig. 4E). These results suggest that expression of $Myh10^{DN}$ inhibits both convergence and extension, as observed by the increase in cell density, and cell growth, based on the decreased lumenal surface areas of cells within the prosensory region.

The strong expression of MYH10 and MYH14 in IPCs suggested that the development of these cells might be specifically regulated by myosin II. To examine this possibility, the IPC region was visualized at the midpoint of the cochlea in control and $Myh10^{DN}$ experimental cochleae. Results indicated an increase in the number of cells within the IPC region in cochleae from experimental embryos (76.5 IPCs/100 μm in $Myh10^{DN}$ experimental versus 32.2 IPCs/100 μm in control, P=0.004; Fig. 4F-I). In addition, all of these cells retained a rounded morphology rather than a cuboidal or elongated shape. The identity of these cells as IPCs was confirmed by labeling with the IPC marker $p75^{NTR}$ (Fig. 4J,K). However, a similar analysis in the more mature basal region of the cochlea in both control and experimental cochleae indicated a progressive improvement in overall cellular patterning in the $Myh10^{DN}$ cochleae, suggesting a delay, rather than a complete disruption, in cellular patterning (data not shown). These results suggest that the $Myh10^{DN}$ allele does not completely inhibit the activity of myosin II.

Finally, to determine whether a disruption in radial intercalation could contribute to the patterning defects observed in $Myh10^{DN}$ cochleae, the thickness of the epithelium along the basolumenal axis was examined in cross sections from wild type and $Myh10^{DN}$ mutants. No change in epithelial thickness was observed (see Fig. S4 in the supplementary material), suggesting that radial intercalation was not affected in $Myh10^{DN}$ mutants.

Pharmacological inhibition of myosin II function inhibits extension of the sensory epithelium

As the extent of the dominant negative activity of $Myh10^{DN}$ has not been determined, we sought to further examine the effects of inhibition of myosin II in cochlear explant cultures using three different myosin II antagonists: blebbistatin, which selectively inhibits myosin II (Straight et al., 2003; Limouze et al., 2004; Kovacs et al., 2004); the RHO-associated protein kinase (ROCK) inhibitor, Y27632 (Kimura et al., 1996; Amano et al., 1996; Uehata et al., 1997); and ML7, an inhibitor of myosin light chain kinase (Wadgaonkar et al., 2005; Bessard et al., 2006). Effects of inhibition of myosin II on cochlear extension were quantified using a previously described in vitro outgrowth assay (Wang et al., 2005) (see Materials and methods for details). In control explants, the average extension of the sensory epithelium was ~600 μm (Fig. 5A,B,G). By contrast, treatment with blebbistatin (Fig. 5C) or Y27632 (Fig. 5D) resulted in a significant inhibition of extension by comparison with no treatment or exposure to either N-benzyl-p-toluene sulfonamide (BTS), a specific inhibitor of skeletal muscle myosin (Cheung et al., 2002), or to ML7 (Fig. 5G and data not shown). At 10 μM of blebbistatin, the highest tolerable concentration, extension of the sensory epithelium was reduced to ~150 μm, a 75% reduction from control sensory epithelium (Fig. 5G). In contrast with extension, the width of the sensory epithelium was only significantly increased in explants treated with the highest dose (10 μM) of blebbistatin (Fig. 5H). These results are consistent with the phenotypic changes observed in $Myh10^{DN}$ mutant cochleae. Disruptions in cellular patterning in blebbistatin-treated explants

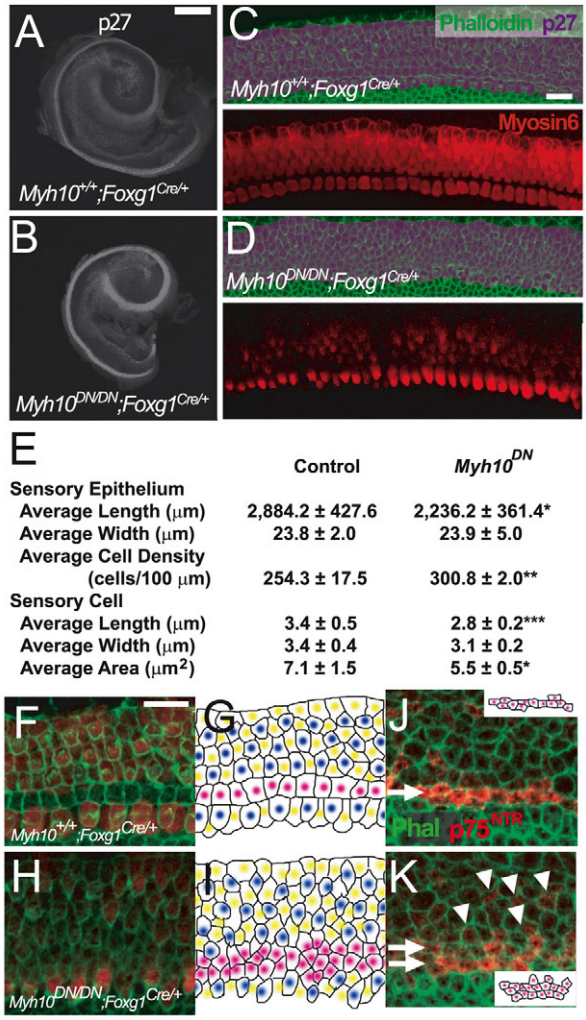

Fig. 4. *Myh10*^{DN} inhibits CE and disrupts cellular patterning. (**A**,**B**) Whole mounts of E16 cochleae from a control (A) and an *Myh10*^{DN} mutant (B). The prosensory domain is marked by p27^{Kip1}. Note that the sensory epithelium appears shorter along the length and wider in the apex in the mutant. (**C**) Upper panel illustrates individual cell boundaries within the developing sensory epithelium (violet) in the middle region of the cochlea from a control embryo at E16. Lower panel illustrates pattern of hair cells (red). (**D**) Similar view as in C, except from an *Myh10*^{DN} mutant. Cellular pattern is disrupted, average cell size appears smaller and expression of myosin 6 is decreased as compared with the control, which could be a result of direct downregulation. Also, alignment of hair cells is disrupted. (**E**) Quantification of changes in morphometric parameters. The length of the sensory epithelium is significantly decreased in *Myh10*^{DN} cochleae but the width is unchanged as a result of a significant increase in cell density. (**F-K**) The sensory epithelium in control and *Myh10*^{DN} cochleae. (F) Fluorescent image of the sensory epithelium in the middle region of the cochlea from an E16 control embryo. Cell borders are labeled with phalloidin (green) and hair cells are marked with anti-myosin 6 (red). (G) Line drawing derived from the image in F, with cell types marked as follows: hair cells, blue; supporting cells, yellow; pillar cells, pink. (H) Comparable image to F, but from an *Myh10*^{DN} cochlea. Note the decreased cell size and disrupted organization. (I) Line drawing as in G. Rather than a single row, multiple rows of pillar cells (pink) are present. (J,K) Sensory epithelium in the middle region of the cochlea from an E16 control (J) and an *Myh10*^{DN} (K) embryo. Inner pillar cells are labeled with anti-p75^{NTR} (red). A single row of inner pillar cells (arrow) is present in the control. Three additional p75^{NTR}-positive cells are present adjacent to the developing inner pillar cell row (just above the arrow). By contrast, two rows of inner pillar cells are present in the mutant (arrows) and additional anti-p75^{NTR}-positive cells (arrowheads) are located in the outer hair cell domain. Insets: line drawings of the inner pillar cells in J and K (not to scale). Scale bars: 200 μm in A,C; 10 μm in B,D,F (same magnification in J,H,K). *P<0.01, **P<0.02, ***P<0.05.

appeared comparable with, but more severe than, the disruptions observed in *Myh10*^{DN} mutants (Fig. 5E,F). In addition to multiple rows of IPCs, outer hair cells and, to a lesser extent, inner hair cells also failed to align into the characteristic one row of inner hair cells and three rows of outer hair cells (Fig. 5E,F). In addition, individual cell length, width and overall area showed decreases that were comparable to those observed in *Myh10*^{DN} mutants (Fig. 5I). Finally, to confirm that treatment with blebbistatin did not lead to a disruption of junctional complexes, expression of the tight junction protein ZO1 (TJP1 – Mouse Genome Informatics) was examined in control and blebbistatin-treated explants (Fig. 5J,K). Although patterning defects are evident in response to blebbistatin, ZO1 is still restricted to the lumenal boundaries of each cell, suggesting that the epithelial integrity is intact.

Inhibition of myosin II leads to changes in inner pillar cell morphology

The analysis of changes in cell morphology had suggested that developing IPCs become more flattened during the period of extension. To determine whether changes in IPC shapes are regulated through myosin II, IPCs were specifically labeled in explants that had been treated with blebbistatin for 48 hours beginning at E14. The overall length of the sensory epithelium was shorter in blebbistatin-treated explants and the row of IPCs was disorganized (Fig. 6). In addition, the lumenal profiles of individual IPCs indicated that inhibition of myosin II resulted in cells that had failed to flatten. Quantification of the lengths and widths of individual IPCs indicated a significant decrease in the length and a significant increase in the width of IPCs in blebbistatin-treated explants (Fig. 6).

Myosin II-dependent extension occurs between E14.5 and E17.5

As discussed above, previous results had suggested that a considerable amount of cochlear convergence and extension occurs between E14 and E16.5. To determine whether the effects of myosin II are limited to this phase of development, cochlear explants were established at E13.5 and treated with blebbistatin for 48 hour time periods beginning after 0, 1, 2 or 4 days in vitro (equivalent to E13.5, E14.5, E15.5 or E17.5; Fig. 7A,B). All explants were fixed after a total of 6 days in vitro. Also, as it was difficult to bisect the cochlea in exactly the same place in each explant, cochleae were established intact and the full extent of the Reissner's membrane was removed to completely expose the sensory epithelium. The presence of an intact sensory epithelium did not appear to significantly affect extension, however, the average width of the sensory epithelium was somewhat wider by comparison with explants that had been bisected (data not shown). Significant shortening and widening of the sensory epithelium was observed when blebbistatin treatment was initiated at either E14.5 or E15.5 (Fig. 7C,D). Initiation of blebbistatin

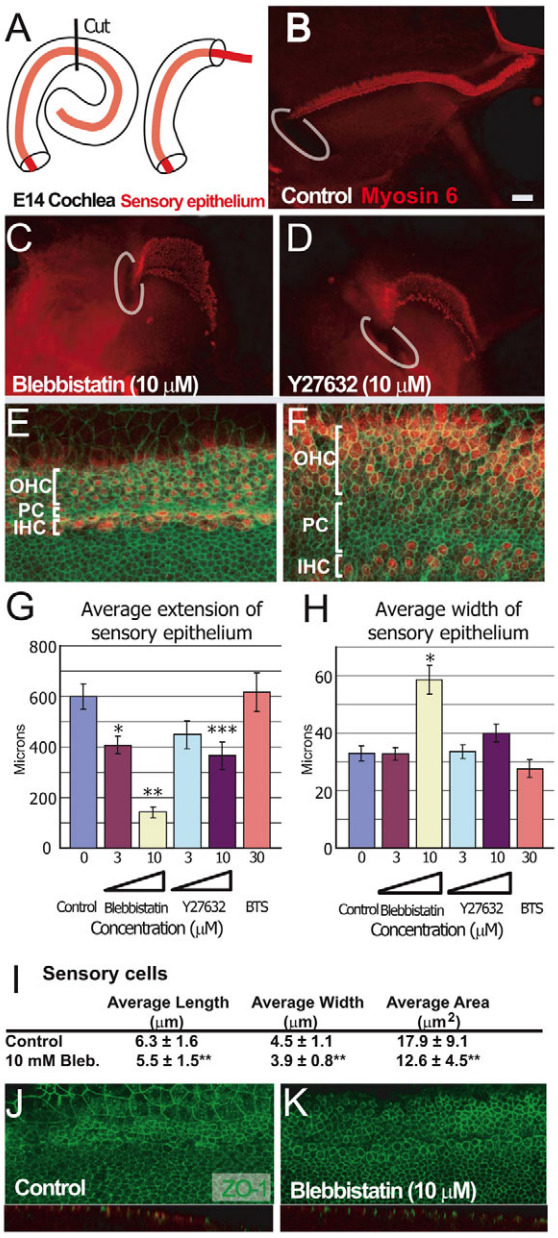

Fig. 5. Inhibition of myosin II activity disrupts cochlear CE. (**A**) Outgrowth of the sensory epithelium was assayed by cutting the intact cochlear duct at its midpoint and then maintaining the basal piece in vitro. Over the subsequent 72-96 hours the sensory epithelium extended outwards from the cut end of the explant. (**B**) Control explant established as described in A. The site of the initial cut is marked in white. The sensory epithelium (hair cells marked in red) extends from the initial cut site. (**C**) Explant established as in B, but treated with 10 μM of the myosin II inhibitor blebbistatin beginning at E14. The sensory epithelium is noticeably shorter and wider. (**D**) An explant established as in B, but treated with 10 μM of the ROCK inhibitor Y27632. The phenotype of the sensory epithelium is similar to that in C. (**E**,**F**) Images of the sensory epithelium from control (E) and 10 μM blebbistatin-treated (F) explants labeled with anti-myosin 6 (red) and phalloidin (green). Additional inner pillar cells (PC) are present in blebbistatin-treated explants. Patterning in the IHCs and OHCs is also disrupted. Abbreviations as in Fig. 2. (**G**) Treatment with either blebbistatin or Y27632 results in a significant and dose-dependent decrease in extension of the sensory epithelium. By contrast, the skeletal muscle myosin inhibitor BTS did not affect extension. (**H**) Treatment with 10 μM blebbistatin leads to a significant increase in the width of the sensory epithelium. However, the width of the sensory epithelium was not significantly increased in explants treated with 10 μM Y27632. (**I**) Blebbistatin treatment leads to changes in cell shape that are consistent with changes in *Myh10*^{DN} mutants. (**J**,**K**) Surface (upper panel) and cross-section (lower panel) views of control (J) and blebbistatin-treated (K) explants labeled with an antibody specific for the tight junction protein ZO1 (green). Tight junctions are present in explants from both conditions and are restricted to the lumenal surfaces. Scale bars: 50 μm in B (same magnification in C,D); 20 μm in E (same magnification in F,I,J). *P<0.005, **P<0.001, ***P<0.01.

treatment at E13.5 did not lead to a significantly shorter sensory epithelium (Fig. 7C), possibly because myosin II-dependent outgrowth does not begin prior to E14.5. By contrast, treatment with blebbistatin between E17.5 and E19.5 did not significantly affect cochlear length, but did result in a significant increase in the width of the sensory epithelium, suggesting that myosin II-dependent extension, but not cellular rearrangement, might be completed by E17.5. Regardless of the timing of blebbistatin addition, the total number of hair cells was unaffected.

Myosin II-dependent extension occurs autonomously in the cochlear epithelium

The results described above suggest that myosin II provides the driving force for extension within the cochlear sensory epithelium. However, in vitro explants also contained mesenchymal cells located beneath the basement membrane of the developing sensory epithelium. Since these cells have been implicated in several aspects of cochlear development, including outgrowth (Phippard et al., 1999), it seemed possible that the outgrowth of the sensory epithelium could be an indirect result of ongoing extension in the associated mesenchyme. Therefore, to determine whether extension of the sensory epithelium occurs autonomously, cochlear explants were established as described in the previous section, with the exception that all underlying mesenchyme was removed at the time of culture (Montcouquiol and Kelley, 2003). Treatment with blebbistatin still significantly inhibited both the lengthening and narrowing of the sensory epithelium (Fig. 7E-H), demonstrating that myosin II directly regulates extension within the sensory epithelium.

DISCUSSION

The results presented here demonstrate that extension between E14 and E16 plays a key role in cochlear patterning. During this time period, the length of the prosensory domain increases by ~70% whereas the width of the domain decreases by ~30%. Moreover, during the same time period, the lumenal surface of each prosensory cell increases by an average of 36%. As a result, prosensory cell density along the long axis of the cochleae decreases by nearly 50%. Since all prosensory cells are postmitotic at this point (Ruben, 1967) and cell death is minimal (Nikolic et al., 2000; Chen et al., 2002), the observed changes in patterning are most likely to be a result of cellular rearrangement. The demonstration that extension is disrupted in response to either genetic or pharmacological inhibition of myosin II indicates a crucial role for this molecule.

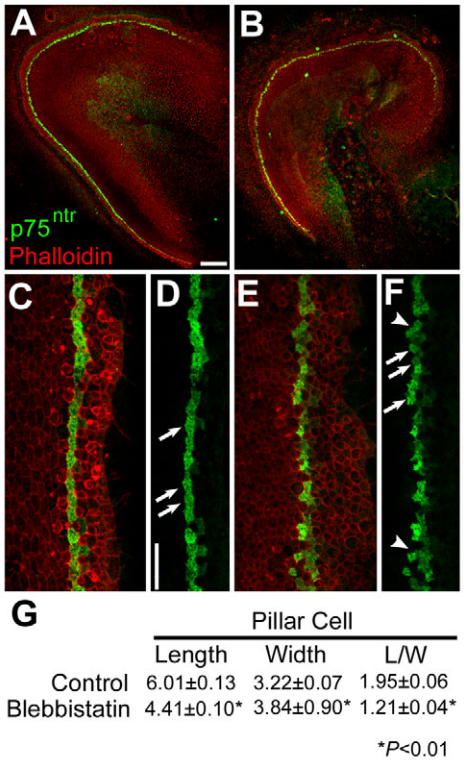

Fig. 6. Pillar cell shape is affected in blebbistatin-treated cochlear explants. (**A**) Low magnification view of a control explant established at E13 and fixed after 72 hours in vitro. The pillar cells (green) extend in a single line along the length of the explant. (**B**) Low magnification view of an explant established and labeled as in A, but treated with 10 μM blebbistatin for 48 hours beginning after 24 hours in vitro. The overall length of the epithelium is shorter and the row of pillar cells appears less organized. (**C**) High magnification view of the sensory epithelium from a control explant labeled as in A. The pillar cells are present in a single organized row. (**D**) The same view as in C with the red channel removed. Pillar cells are indicated (arrows). (**E**) High magnification view of the sensory epithelium from an explant treated with 10 μM blebbistatin, labeled as in A. (**F**) The same view as in E, with the red channel removed. Note the poor organization of the row of pillar cells and the more rounded shape. (**G**) Quantification of the average length and width of pillar cells in control and blebbistatin-treated explants. In blebbistatin-treated explants, pillar cell lengths are significantly shorter, whereas pillar cell widths are significantly greater, resulting in a significant decrease in the length/width ratio. Scale bars: 100 μm in A (same magnification in B); 20 μm in D (same magnification in C,E,F).

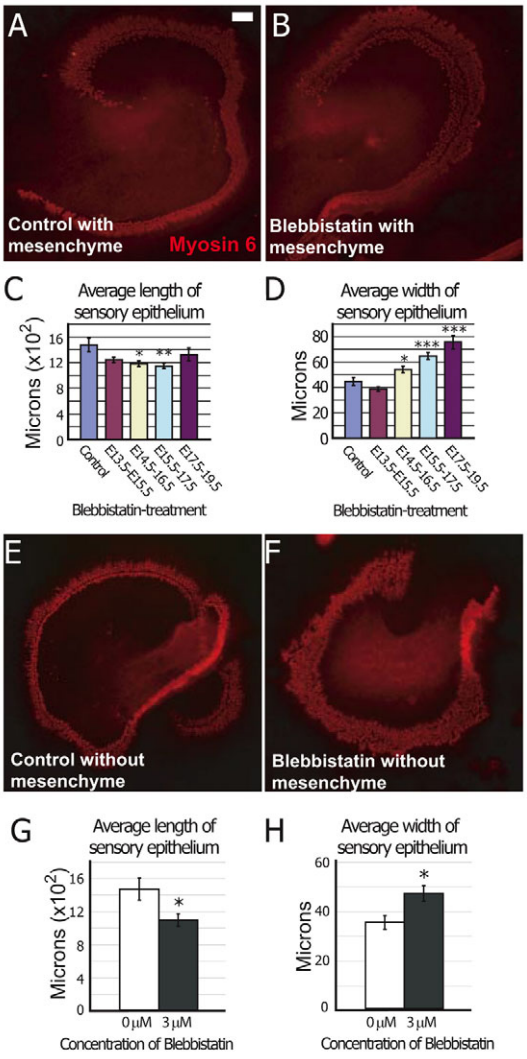

Fig. 7. CE occurs autonomously within the sensory epithelium. (**A**,**B**) Control (A) and 10 μM blebbistatin (B) explants treated for 48 hours beginning at E14.5. Hair cells are labeled with anti-myosin 6, the sensory epithelium is shorter and wider in the blebbistatin-treated explant. (**C**,**D**) Lengths and widths for cochlear explants treated with 10 μM blebbistatin during the indicated time periods. Treatment beginning at E14.5 or E15.5 results in significant shortening and widening of the sensory epithelium. Treatment beginning at E17.5 results in a significant widening without a change in length. (**E**,**F**) Control (E) and 3 μM blebbistatin-treated (F) explants established without mesenchyme. The effects of blebbistatin are similar to those observed in explants with mesenchyme. (**G**,**H**) Effects of blebbistatin on the length and width of the sensory epithelium are comparable between explants with and without mesenchyme. Scale bar: 50 μm in A (same magnification in B,E,F). *P<0.05, **P<0.01, ***P<0.001.

The specific morphological changes and cellular rearrangements that are mediated through myosin II are not clear. MYH10 and MYH14 are asymmetrically distributed between different cell types, as well as in different regions of individual cells. In particular, more intense labeling of MYH10 is present on cell membranes oriented parallel to the axis of extension. At these membranes it seems possible that MYH10 could play a role in the elongation of cells along this axis. Results in both *Dictyostelium* and *Xenopus* have suggested that myosin II, and in particular myosin IIB (MYH10) plays a key role in regulating changes in cell shape through its role as an actin crosslinker (Egelhoff et al., 1996; Laevsky and Knecht, 2003; Rolo et al., 2009). Morpholino-based inhibition of myosin IIB in *Xenopus* neural tube leads to defects in neural tube closure as a result of defects in cell shape change (Rolo et al., 2009). Similar defects were observed in these studies, suggesting a potential similar role for myosin II in the cochlea.

In addition, mutations in *zipper* (*Drosophila* myosin II) have been shown to lead to disruptions in the formation of boundaries in the imaginal disc and ommatidia (Major and Irvine, 2006; Fiehler and Wolff, 2007), and mutations in *Myh10* in mice lead to hydrocephalus as a result of disruptions in the ventricular layer boundary (Ma et al.,

2007). MYH10 and MYH14 are distributed at boundaries between different cell types within the OC, and the alignments of these cell types was affected in blebbistatin-treated explants and, to a lesser extent, in *Myh10*^{DN} mutants. The specific role of myosin II in boundary formation is unclear. However, its ability to regulate contractile tension along F-actin cables through crosslinking has been implicated (Major and Irvine, 2006; Ma et al., 2007).

Myosin II has also been shown to regulate CE during germband extension in *Drosophila* through modulation of junctional remodeling (Bertet et al., 2004; Zallen and Wieschaus, 2004). In particular, cell-cell junctions oriented perpendicular to the axis of extension are actively eliminated, whereas junctions oriented parallel are actively developed or increased. The distribution of MYH proteins in the developing cochlea was inconsistent with a similar role for myosin II in junctional remodeling. However, the changes in the distribution of pillar cells in cochleae in which myosin II function was perturbed suggest that some amount of junctional remodeling does occur.

Short cochleae and cellular patterning defects are also observed in animals with mutations in PCP genes, such as *Vangl2* or dishevelled (Montcouquiol et al., 2003; Wang et al., 2005; Wang et al., 2006). The similarities in the phenotypes suggest that PCP and myosin II could function in the same signaling pathway. This possibility is supported by data indicating interactions between PCP and myosin II in *Drosophila* ommatidial rotation (Winter et al., 2001). Conversely, CE in the developing *Drosophila* germband is dependent on myosin II but is apparently not regulated through the PCP pathway, as Frizzled and Dishevelled are not required for extension in this system (Zallen and Wieschaus, 2004). This raises the possibility that the similar cochlear phenotypes are not a result of perturbations in a single pathway and instead occur because of disruption of distinct pathways that result in similar phenotypes. Shortened cochleae have also been observed in humans with Mondini dysplasia, often caused by mutations in the anion transporter *SLC26A4* (Campbell et al., 2001), and in mice in response to targeted removal or disruption of multiple genes expressed within the inner ear, including *Foxg1*, neurogenin 1, *Pou3f4* and *Gli3* (Phippard et al., 1999; Ma et al., 2000; Pauley et al., 2006; Qian et al., 2007; Bok et al., 2007). None of these genes has been implicated in PCP, suggesting that other pathways mediate other aspects of cochlear elongation. At this point, it is not possible to determine whether myosin II functions through a PCP-dependent or independent pathway, however, analysis of myosin II distributions in PCP mutants will be informative.

One of the more intriguing results of this study was the observation that morphological changes consistent with convergence and extension were largely restricted to the developing IPC and outer hair cell regions (compare changes in Fig. 3 with those described in Bertet et al. (Bertet et al., 2004). These results suggest that cochlear extension is probably asymmetric. Convergence apparently occurs predominantly, or exclusively, from the lateral side, with all cells moving towards a boundary that is established between the inner hair cells and IPCs.

In conclusion, the results presented here demonstrate a role for myosin II in the outgrowth and patterning of the developing sensory epithelium, as well as in changes in the shape and size of the lumenal surface areas of individual prosensory cells. MYH10 and MYH14 are distributed in patterns that are suggestive of multiple roles in cochlear development, including CE and the establishment of cell-cell boundaries. In addition, disruptions in myosin II activity through either genetic or pharmacological methods result in shorter cochleae with marked defects in cellular patterning. Finally, analysis of changes in cell shape and position indicate that cellular convergence within the sensory epithelium is not symmetric, with more pronounced changes in cell shape occurring in the lateral (IPC and outer hair cell) region. These results identify myosin II as a key regulator of cellular patterning within the cochlea and provide intriguing new insights into the morphological changes that are required for the development of this rigorously patterned epithelium.

The authors wish to acknowledge the excellent technical assistance of Weise Chang. This project was supported by funds from the NIH Intramural program to R.S.A. and M.W.K. and by grants from the JSPS Research Fellowship for Japanese Biomedical and Behavioral Researchers at NIH to N.Y. and T.O. Deposited in PMC for release after 12 months.

Supplementary material

Supplementary material for this article is available at http://dev.biologists.org/cgi/content/full/136/12/1977/DC1

References

Amano, M., Ito, M., Kimura, K., Fukata, Y., Chihara, K., Nakano, T., Matsuura, Y. and Kaibuchi, K. (1996). Phosphorylation and activation of myosin by Rho-associated kinase (Rho-kinase). *J. Biol. Chem.* **271**, 20246-20249.

Bertet, C., Sulak, L. and Lecuit, T. (2004). Myosin-dependent junction remodelling controls planar cell intercalation and axis elongation. *Nature* **429**, 667-671.

Bessard, A., Coutant, A., Rescan, C., Ezan, F., Fremin, C., Courselaud, B., Ilyin, G. and Baffet, G. (2006). An MLCK-dependent window in late G1 controls S phase entry of proliferating rodent hepatocytes via ERK-p70S6K pathway. *Hepatology* **44**, 152-163.

Bok, J., Dolson, D. K., Hill, P., Ruther, U., Epstein, D. J. and Wu, D. K. (2007). Opposing gradients of Gli repressor and activators mediate Shh signaling along the dorsoventral axis of the inner ear. *Development* **134**, 1713-1722.

Campbell, C., Cucci, R. A., Prasad, S., Green, G. E., Edeal, J. B., Galer, C. E., Karniski, L. P., Sheffield, V. C. and Smith, R. J. (2001). Pendred syndrome, DFNB4, and PDS/SLC26A4 identification of eight novel mutations and possible genotype-phenotype correlations. *Hum. Mutat.* **17**, 403-411.

Cantos, R., Cole, L. K., Acampora, D., Simeone, A. and Wu, D. K. (2000). Patterning of the mammalian cochlea. *Proc. Natl. Acad. Sci. USA* **97**, 11707-11713.

Chen, A. H., Ni, L., Fukushima, K., Marietta, J., O'Neill, M., Coucke, P., Willems, P. and Smith, R. J. (1995). Linkage of a gene for dominant non-syndromic deafness to chromosome 19. *Hum. Mol. Genet.* **4**, 1073-1076.

Chen, P. and Segil, N. (1999). p27(Kip1) links cell proliferation to morphogenesis in the developing organ of Corti. *Development* **126**, 1581-1590.

Chen, P., Johnson, J. E., Zoghbi, H. Y. and Segil, N. (2002). The role of Math1 in inner ear development: Uncoupling the establishment of the sensory primordium from hair cell fate determination. *Development* **129**, 2495-2505.

Cheung, A., Dantzig, J. A., Hollingworth, S., Baylor, S. M., Goldman, Y. E., Mitchison, T. J. and Straight, A. F. (2002). A small-molecule inhibitor of skeletal muscle myosin II. *Nat. Cell Biol.* **4**, 83-88.

Conti, M. A. and Adelstein, R. S. (2008). Nonmuscle myosin II moves in new directions. *J. Cell Sci.* **121**, 11-18.

Conti, M. A., Even-Ram, S., Liu, C., Yamada, K. M. and Adelstein, R. S. (2004). Defects in cell adhesion and the visceral endoderm following ablation of nonmuscle myosin heavy chain II-A in mice. *J. Biol. Chem.* **279**, 41263-41266.

Donaudy, F., Snoeckx, R., Pfister, M., Zenner, H. P., Blin, N., Di Stazio, M., Ferrara, A., Lanzara, C., Ficarella, R., Declau, F. et al. (2004). Nonmuscle myosin heavy-chain gene MYH14 is expressed in cochlea and mutated in patients affected by autosomal dominant hearing impairment (DFNA4). *Am. J. Hum. Genet.* **74**, 770-776.

Egelhoff, T. T., Naismith, T. V. and Brozovich, F. V. (1996). Myosin-based cortical tension in Dictyostelium resolved into heavy and light chain-regulated components. *J. Muscle Res. Cell Motil.* **17**, 269-274.

Fiehler, R. W. and Wolff, T. (2007). Drosophila Myosin II, Zipper, is essential for ommatidial rotation. *Dev. Biol.* **310**, 348-362.

Golomb, E., Ma, X., Jana, S. S., Preston, Y. A., Kawamoto, S., Shoham, N. G., Goldin, E., Conti, M. A., Sellers, J. R. and Adelstein, R. S. (2004). Identification and characterization of nonmuscle myosin II-C, a new member of the myosin II family. *J. Biol. Chem.* **279**, 2800-2808.

Heath, K. E., Campos-Barros, A., Toren, A., Rozenfeld-Granot, G., Carlsson, L. E., Savige, J., Denison, J. C., Gregory, M. C., White, J. G., Barker, D. F. et al. (2001). Nonmuscle myosin heavy chain IIA mutations define a spectrum of autosomal dominant macrothrombocytopenias: May-Hegglin anomaly and Fechtner, Sebastian, Epstein, and Alport-like syndromes. *Am. J. Hum. Genet.* **69**, 1033-1045.

Hebert, J. M. and McConnell, S. K. (2000). Targeting of cre to the Foxg1 (BF-1) locus mediates loxP recombination in the telencephalon and other developing head structures. *Dev. Biol.* **222**, 296-306.
Irvine, K. D. and Wieschaus, E. (1994). Cell intercalation during Drosophila germband extension and its regulation by pair-rule segmentation genes. *Development* **120**, 827-841.
Itoh, K. and Adelstein, R. S. (1995). Neuronal cell expression of inserted isoforms of vertebrate nonmuscle myosin heavy chain II-B. *J. Biol. Chem.* **270**, 14533-14540.
Jacobson, A. G. and Gordon, R. (1976). Changes in the shape of the developing vertebrate nervous system analyzed experimentally, mathematically and by computer simulation. *J. Exp. Zool.* **197**, 191-246.
Jacques, B. E., Montcouquiol, M. E., Layman, E. M., Lewandoski, M. and Kelley, M. W. (2007). Fgf8 induces pillar cell fate and regulates cellular patterning in the mammalian cochlea. *Development* **134**, 3021-3029.
Kamm, K. E. and Stull, J. T. (1985). The function of myosin and myosin light chain kinase phosphorylation in smooth muscle. *Annu. Rev. Pharmacol. Toxicol.* **25**, 593-620.
Keller, R. E. (1986). The cellular basis of amphibian gastrulation. *Dev. Biol. (NY 1985)* **2**, 241-327.
Keller, R. (2002). Shaping the vertebrate body plan by polarized embryonic cell movements. *Science* **298**, 1950-1954.
Keller, R., Davidson, L., Edlund, A., Elul, T., Ezin, M., Shook, D. and Skoglund, P. (2000). Mechanisms of convergence and extension by cell intercalation. *Philos. Trans. R. Soc. Lond. B Biol. Sci.* **355**, 897-922.
Kim, K. Y., Kovacs, M., Kawamoto, S., Sellers, J. R. and Adelstein, R. S. (2005). Disease-associated mutations and alternative splicing alter the enzymatic and motile activity of nonmuscle myosins II-B and II-C. *J. Biol. Chem.* **280**, 22769-22775.
Kimura, K., Ito, M., Amano, M., Chihara, K., Fukata, Y., Nakafuku, M., Yamamori, B., Feng, J., Nakano, T., Okawa, K. et al. (1996). Regulation of myosin phosphatase by Rho and Rho-associated kinase (Rho-kinase). *Science* **273**, 245-248.
Kovacs, M., Toth, J., Hetenyi, C., Malnasi-Csizmadia, A. and Sellers, J. R. (2004). Mechanism of blebbistatin inhibition of myosin II. *J. Biol. Chem.* **279**, 35557-35563.
Laevsky, G. and Knecht, D. A. (2003). Cross-linking actin filaments by myosin II is a major contributor to cortical intergrity and cell motility in restrictive environments. *J. Cell Sci.* **116**, 3761-3770.
Lalwani, A. K., Linthicum, F. H., Wilcox, E. R., Moore, J. K., Walters, F. C., San Agustin, T. B., Mislinski, J., Miller, M. R., Sinninger, Y., Attaie, A. et al. (1997). A five-generation family with late-onset progressive hereditary hearing impairment due to cochleosaccular degeneration. *Audiol. Neurootol.* **2**, 139-154.
Lalwani, A. K., Goldstein, J. A., Kelley, M. J., Luxford, W., Castelein, C. M. and Mhatre, A. N. (2000). Human nonsyndromic hereditary deafness DFNA17 is due to a mutation in nonmuscle myosin MYH9. *Am. J. Hum. Genet.* **67**, 1121-1128.
Limouze, J., Straight, A. F., Mitchison, T. and Sellers, J. R. (2004). Specificity of blebbistatin, an inhibitor of myosin II. *J. Muscle Res. Cell Motil.* **25**, 337-341.
Ma, Q., Anderson, D. J. and Fritzsch, B. (2000). Neurogenin 1 null mutant ears develop fewer, morphologically normal hair cells in smaller sensory epithelia devoid of innervation. *J. Assoc. Res. Otolaryngol.* **1**, 129-143.
Ma, X., Kawamoto, S., Hara, Y. and Adelstein, R. S. (2004). A point mutation in the motor domain of nonmuscle myosin II-B impairs migration of distinct groups of neurons. *Mol. Biol. Cell* **15**, 2568-2579.
Ma, X., Bao, J. and Adelstein, R. S. (2007). Loss of cell adhesion causes hydrocephalus in nonmuscle myosin II-B-ablated and mutated mice. *Mol. Biol. Cell* **18**, 2305-2312.
Major, R. J. and Irvine, K. D. (2006). Localization and requirement for Myosin II at the dorsal-ventral compartment boundary of the Drosophila wing. *Dev. Dyn.* **235**, 3051-3058.
McKenzie, E., Krupin, A. and Kelley, M. W. (2004). Cellular growth and rearrangement during the development of the mammalian organ of Corti. *Dev. Dyn.* **229**, 802-812.
Montcouquiol, M. and Kelley, M. W. (2003). Planar and vertical signals control cellular differentiation and patterning in the mammalian cochlea. *J. Neurosci.* **23**, 9469-9478.
Montcouquiol, M., Rachel, R. A., Lanford, P. J., Copeland, N. G., Jenkins, N. A. and Kelley, M. W. (2003). Identification of Vangl2 and Scrb1 as planar polarity genes in mammals. *Nature* **423**, 173-177.
Nikolic, P., Jarlebark, L. E., Billett, T. E. and Thome, P. R. (2000). Apoptosis in the developing rat cochlea and its related structures. *Dev. Brain Res.* **119**, 75-83.
Pauley, S., Lai, E. and Fritzsch, B. (2006). Foxg1 is required for morphogenesis and histogenesis of the mammalian inner ear. *Dev. Dyn.* **235**, 2470-2482.
Phippard, D., Lu, L., Lee, D., Saunders, J. C. and Crenshaw, E. B., III (1999). Targeted mutagenesis of the POU-domain gene Brn4/Pou3f4 causes developmental defects in the inner ear. *J. Neurosci.* **19**, 5980-5989.
Qian, D., Jones, C., Rzadzinska, A., Mark, S., Zhang, X., Steel, K. P., Dai, X. and Chen, P. (2007). Wnt5a functions in planar cell polarity regulation in mice. *Dev. Biol.* **306**, 121-133.
Rolo, A., Skoglund, P. and Keller, R. (2009). Morphogenetic movements driving neural tube closure in Xenopus require myosin IIB. *Dev. Biol.* **327**, 327-338.
Ruben, R. J. (1967). Development of the inner ear of the mouse: a radioautographic study of terminal mitoses. *Acta Otolaryngol*, Suppl. **220**,1-44.
Sellers, J. R. (2000). Myosins: a diverse superfamily. *Biochim. Biophys. Acta* **1496**, 3-22.
Skoglund, P., Rolo, A., Chen, X., Gumbiner, B. M. and Keller, R. (2008). Convergence and extension at gastrulation require a myosin IIB-dependent cortical actin network. *Development* **135**, 2435-2444.
Straight, A. F., Cheung, A., Limouze, J., Chen, I., Westwood, N. J., Sellers, J. R. and Mitchison, T. J. (2003). Dissecting temporal and spatial control of cytokinesis with a myosin II Inhibitor. *Science* **299**, 1743-1747.
Tullio, A. N., Accili, D., Ferrans, V. J., Yu, Z. X., Takeda, K., Grinberg, A., Westphal, H., Preston, Y. A. and Adelstein, R. S. (1997). Nonmuscle myosin II-B is required for normal development of the mouse heart. *Proc. Natl. Acad. Sci. USA* **94**, 12407-12412.
Uehata, M., Ishizaki, T., Satoh, H., Ono, T., Kawahara, T., Morishita, T., Tamakawa, H., Yamagami, K., Inui, J., Maekawa, M. et al. (1997). Calcium sensitization of smooth muscle mediated by a Rho-associated protein kinase in hypertension. *Nature* **389**, 990-994.
von Bekesy, G. (1949). The vibration of the cochlear partition in anatomical preparations and in models of the inner ear. *J. Acoust. Soc. Am.* **21**, 233-245.
Wadgaonkar, R., Linz-McGillem, L., Zaiman, A. L. and Garcia, J. G. (2005). Endothelial cell myosin light chain kinase (MLCK) regulates TNFalpha-induced NFkappaB activity. *J. Cell. Biochem.* **94**, 351-364.
Wang, J., Mark, S., Zhang, X., Qian, D., Yoo, S. J., Radde-Gallwitz, K., Zhang, Y., Lin, X., Collazo, A., Wynshaw-Boris, A. et al. (2005). Regulation of polarized extension and planar cell polarity in the cochlea by the vertebrate PCP pathway. *Nat. Genet.* **37**, 980-985.
Wang, J., Hamblet, N. S., Mark, S., Dickinson, M. E., Brinkman, B. C., Segil, N., Fraser, S. E., Chen, P., Wallingford, J. B. and Wynshaw-Boris, A. (2006). Dishevelled genes mediate a conserved mammalian PCP pathway to regulate convergent extension during neurulation. *Development* **133**, 1767-1778.
Winter, C. G., Wang, B., Ballew, A., Royou, A., Karess, R., Axelrod, J. D. and Luo, L. (2001). Drosophila Rho-associated kinase (Drok) links Frizzled-mediated planar cell polarity signaling to the actin cytoskeleton. *Cell* **105**, 81-91.
Yabe, D., Komuro, R., Liang, G., Goldstein, J. L. and Brown, M. S. (2003). Liver-specific mRNA for Insig-2 down-regulated by insulin: implications for fatty acid synthesis. *Proc. Natl. Acad. Sci. USA* **100**, 3155-3160.
Yang, T., Pfister, M., Blin, N., Zenner, H. P., Pusch, C. M. and Smith, R. J. (2005). Genetic heterogeneity of deafness phenotypes linked to DFNA4. *Am. J. Med. Genet. A* **139**, 9-12.
Zallen, J. A. and Wieschaus, E. (2004). Patterned gene expression directs bipolar planar polarity in Drosophila. *Dev. Cell* **6**, 343-355.